Spontaneous Helix Hand Reversal and Tendril Perversion in Climbing Plants

Alain Goriely[1,2,*] and Michael Tabor[1]
[1]*University of Arizona, Program in Applied Mathematics, Building #89, Tucson, Arizona 85721*
[2]*Université Libre de Bruxelles, Département de Mathématique, CP218/1, 1050 Brussels, Belgium*
(Received 4 November 1997)

The helix hand reversal exhibited by the tendrils of climbing plants when attached to a support is investigated. Modeled as a thin elastic rod with intrinsic curvature, a linear and nonlinear stability analysis shows the problem to be a paradigm for curvature induced morphogenesis in which symmetry breaking is constrained by a global invariant. [S0031-9007(98)05309-5]

PACS numbers: 87.45.–k

The interesting phenomenon of helix hand reversal, namely, the spontaneous switching of a helical structure of one handedness to its mirror image, can be found in many different guises and was first called *perversion* by the 19th century topologist Listing, presumably after the usage of the word *perversus* to describe inverted seashell specimens in choncology. Its occurrence in climbing plants provides a beautiful mechanical system with which to study the problem of symmetry breaking constrained by a global invariant; total twist in this case. Moreover, we show here that the key mechanical quantity driving the process is the *intrinsic curvature* of the filament (i.e., the curvature of the filament in its lowest relaxed energy state). It is important to note that many filamentary shapes in biology are driven by intrinsic twist (such as the formation of bacterial macrofibers or DNA [1]), whereas tendril perversion provides an example of a different scenario for the shape formation, namely, intrinsic curvature driven morphogenesis. Indeed, the twist-to-writhe conversion argument, usually used to explain the coiling of filaments through energy relaxation [2], does not apply here as the filaments are twistless.

Among the many different mechanisms climbing plants use to climb and grow along supports, the so-called "tendril bearers" or "clingers" constitute an important class (e.g., the grape vine, the hop, the bean, and the melon). Tendrils are tender, soft, curly, and flexible organs whose circumnutation allows the plant to find a support. When a tendril touches a support, such as a trellis, its tissues develop in such a way that it starts to curl and tighten up, eventually becoming robust and tough. This curling provides the plant with an elastic springlike connection to the support that enables it to resist high winds and loads. Since neither the stem nor the support can rotate, the total twist in the tendril cannot change. Therefore, as the tendril curls on itself, the coils of the spiral are reversed at some point so that the tendril goes from a left-handed helix to a right-handed one, the two being separated by a small segment (see Fig. 1).

Tendril perversion fascinated Darwin and he described it at length in his delightful little book *The Movements and Habits of Climbing Plants* [3] based on an essay presented at the Linnean Society in 1865. Thanks to his stimulus, the subject attracted the interest of eminent 19th century biologists such as Gray, de Vries, and Sachs. Interestingly enough, Darwin himself appears to have been unaware of the earlier history of the topic; in particular, it was studied by Léon in 1858, Dutrochet in 1844, and von Mohl and de Candolle in 1827. In fact, de Candolle himself attributes the first observation of the phenomenon to Ampère in the late 18th century. Furthermore a careful examination of the tendrils drawings (Tabula V) of Linné in *Philosophia Botannica* clearly shows a spiral inversion and seems to indicate that Linné was well aware of the phenomenon as early as 1751.

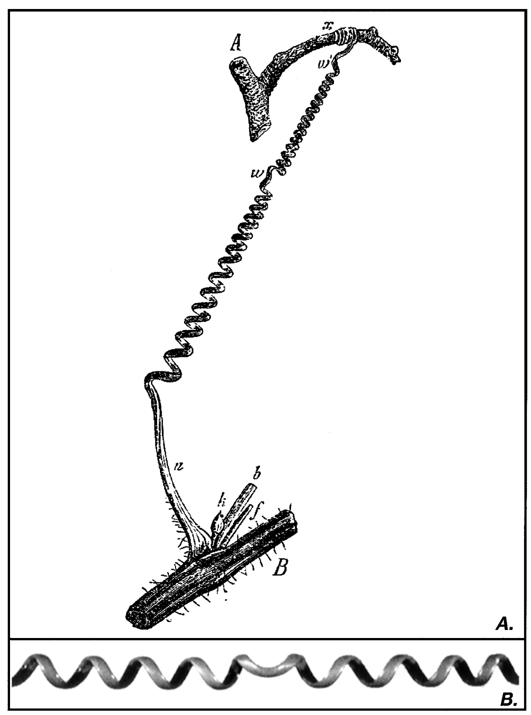

FIG. 1. (a) Tendril perversion in *Bryonia dioica.* Illustration from Sachs' *Text-book of Botany* [11]; (b) perversion in a telephone cord. The effect is achieved by fully stretching out and untwisting the cord and then slowly bringing the ends together.

The equivalent of tendril perversion is nowadays recognized to occur in problems ranging from the false-twist technique in the textile industry [4] to the microscopic properties of biological fibers such as cotton [5] or the formation of bacterial macrofibers [6]. Spiral inversion can also be found in the macrophage scavenger protein, a triple helix with reversed handedness [7], but its most familiar occurrence is to be found in modern telephone cords. As a coiled telephone cord is first extended and completely untwisted and then slowly released, a spiral inversion will naturally appear, usually producing annoying snarls.

Here we give a qualitative and quantitative description of the spiral inversion problem. Many questions readily come to mind: What triggers the phenomenon? What is the associated dynamics? Can it be understood in terms of an instability of certain solutions to the elastic filament equations? The theory of thin elastic rods provides a natural framework to answer these questions. We show that tendril perversion (and more generally the phenomenon of spiral inversion) can be understood through a dynamical analysis of the solutions to the Kirchhoff equations for thin elastic rods.

Consider first a simple space curve x, parametrized by arc length s, whose position may vary in time; i.e., $x = x(s,t)$. [In what follows, $()'$ and $(\dot{})$ denote, respectively, s and t differentiation.] A *local basis* $d_i = d_i(s,t)$, $i = 1,2,3$ is defined by $d_3 = x'(s,t)$, and d_1, d_2 two unit vectors in the plane normal to d_3 such that (d_1, d_2, d_3) forms a right-handed orthonormal basis. There exist a *twist vector* $\kappa = \kappa_1 d_1 + \kappa_2 d_2 + \kappa_3 d_3$ and a *spin vector* $\omega = \omega_1 d_1 + \omega_2 d_2 + \omega_3 d_3$ defining the space and time evolution of the basis along the curve via the *spin and twist equations:*

$$d_i' = \kappa \times d_i, \qquad \dot{d}_i = \omega \times d_i, \qquad i = 1,2,3. \quad (1)$$

Given $\kappa = \kappa(s,t)$ and $\omega = \omega(s,t)$ the curve can be obtained by first solving (1) and then integrating d_3. If d_1 is the normal vector to the curve then the local basis reduces to the well-known Frenet frame.

The Kirchhoff model of rod dynamics describes inextensible rods whose length is much greater than the cross sectional radius. Using these fundamental assumptions, all the physical quantities associated with the filament are averaged over the cross sections and attached to the central axis. The total force $F = F(s,t)$ and moment $M = M(s,t)$ can then be expressed in terms of the local basis. The conservation of linear and angular momentum leads to the Kirchhoff equations which, in scaled variables and for a rod of circular cross section, are [8]

$$F'' = \ddot{d}_3, \quad (2)$$

$$M' + d_3 \times F = d_1 \times \ddot{d}_1 + d_2 \times \ddot{d}_2, \quad (3)$$

$$M = (\kappa_1 - \kappa_1^{(u)})d_1 + (\kappa_2 - \kappa_2^{(u)})d_2 + \Gamma(\kappa_3 - \kappa_3^{(u)})d_3. \quad (4)$$

The last equation is the constitutive relationship of linear elasticity theory in which the parameter $\Gamma = 1/(1+\sigma)$ (where σ is the Poisson ratio) measures the ratio between bending and twisting coefficients of the rod. The intrinsic curvature vector $\kappa^{(u)}$ corresponds to the configuration with the lowest elastic energy; namely, $\mathcal{E} = \frac{1}{2}\int_0^L M \cdot (\kappa - \kappa^{(u)})\, ds$, such that $\mathcal{E} = 0$ when $\kappa = \kappa^{(u)}$. The Frenet curvature is given by $\kappa_F = \sqrt{\kappa_1^2 + \kappa_2^2}$, whereas κ_3 contains information both on the twist of the filament and the Frenet torsion. Here we consider only the effect of a constant intrinsic curvature; that is, we set $\kappa^{(u)} = (K, 0, 0)$, where K is the intrinsic curvature.

In order to understand and analyze spiral inversion, we start with a simple stationary solution: a straight twistless filament under tension $f_3 = \phi^2$ with intrinsic curvature K. As the tension is slowly released, experience shows that there is a critical tension for which the straight filament loses its stability and bifurcates into new solutions. In order to capture this bifurcation and analyze its dynamics we use recently developed methods to study the linear and nonlinear stability of stationary solutions [9,10].

The basic idea consists of expanding the local basis $d = d^{(0)} + \epsilon d^{(1)} + \epsilon^2 d^{(2)} + \ldots$ in a small parameter ϵ and requiring that to each order in ϵ, the basis $d = d(s,t)$ is orthonormal. Since all the relevant geometric and physical quantities are expressed in the local basis, this requirement allows us to expand all quantities in ϵ:

$$\begin{aligned} d_i &= d_i^{(0)} + \epsilon\alpha^{(1)} \times d_i^{(0)} + O(\epsilon^2), \qquad i = 1,2,3, \\ F &= f_i^{(0)} d_i^{(0)} + \epsilon[f_i^{(1)} + (\alpha^{(1)} \times f^{(0)})_i] d_i^{(0)} + O(\epsilon^2), \\ \kappa &= \kappa^{(0)} + (\alpha^{(1)})' + \kappa^{(0)} \times \alpha^{(1)} + O(\epsilon^2), \\ \omega &= \dot{\alpha}^{(1)} + O(\epsilon^2). \end{aligned} \quad (5)$$

Higher order terms can be generated along the same lines. The new variables $\alpha^{(1)}$ describe the orientation of the perturbed basis with respect to the unperturbed one. Defining the stationary configuration in terms of the (six-dimensional) vector $\mu^{(0)} = (f^{(0)}, \kappa^{(0)})$ a linear system for the first-order correction $\mu^{(1)} = (f^{(1)}, \alpha^{(1)})$ can be obtained by inserting (5) in the Kirchhoff equations and collecting terms in ϵ. In compact form, this system reads

$$\mathcal{L}(\mu^{(0)}) \cdot \mu^{(1)} = 0, \quad (6)$$

where $\mathcal{L}$ is a linear, second-order differential operator in s and t.

We consider here the stationary solution: $\mu^{(0)} = (0, 0, \phi^2, 0, 0, 0)$. The solution [to (6)] can be expressed as a sum of the fundamental solutions:

$$\mu_n^{(1)} = e^{\sigma t}(A_n x_n e^{ins} + A_n^* x_n^* e^{-ins}), \quad (7)$$

where $x_n \in \mathbb{C}^6$, $A_n \in \mathbb{C}$, and the growth rate σ is a solution of the dispersion relations $\Delta(\sigma, n) = 0$, obtained by substituting (7) into (6):

$$\Delta = -n^6(n^2 + \phi^2)[\Gamma(n^2 + \phi^2) - K^2] - n^4(n^2 + \phi^2)[(n^2 + 1)(2\Gamma - K^2) + 2]\sigma^2 - n^2(n^2 + 1)[(n^2 + 1)\Gamma + 4(n^2 + \phi^2)]\phi^4 - 2(n^2 + 1)^2\sigma^6. \tag{8}$$

The critical value of the parameters at which new solutions appear is obtained by solving $\Delta(0, n) = 0$:

$$(K^2 - \Gamma n^2) = \phi^2\Gamma. \tag{9}$$

The analysis of this relationship already provides valuable insight into the stability of the straight filament and different cases can be considered: If the filament is infinite, then for a fixed intrinsic curvature there exists a critical value $\phi_0 = K/\sqrt{\Gamma}$, such that for all $\phi > \phi_0$, the rod is (linearly) stable. For $\phi < \phi_0$ the rod becomes linearly unstable. However, if the filament is finite of length $2\pi L$ and the boundary conditions are chosen in such a way that they are not affected by the perturbation, then the first unstable mode is $n = 1/L$, and the corresponding critical tension is $\phi_1^2 = (L^2K^2 - \Gamma)/L^2\Gamma$. Obviously, $\phi_1 < \phi_0$. As the tension is further decreased, new modes become unstable for the values $\phi_k^2 = (L^2K^2 - k^2\Gamma)/L^2\Gamma$. However, only a finite number of modes can be excited. Indeed, as ϕ decreases the last possible excited mode $k_{\max}$ corresponds to $\phi = 0$, that is, the largest integer less or equal to $KL/\sqrt{\Gamma}$.

The solution corresponding to the nth mode can be easily obtained to second order:

$$x(s,t) = \left(s - X_n^2\frac{\sin(2ns) + 2ns}{2n}, -2KX_n^2\frac{\phi^2\Gamma^2 - K^2(1-\Gamma)\cos^2(ns)}{3\phi^4\Gamma^2 - 7K^2\Gamma\phi^2 + 4K^4}, -2X_n\frac{\sin(ns)}{n}\right) \tag{10}$$

where $X_n = \mathrm{Re}(A_n)$ and the amplitude A is (within the context of the linear analysis) still arbitrary. In order to relate the amplitude of the solution to the control parameter, a (one-mode) nonlinear analysis has to be performed [10]. The main idea is to expand the system to third order in ϵ and find the Fredholm condition for the solution to remain bounded in space. This in turn provides a differential equation for the amplitude A_n and its time derivatives whose stationary states relate the amplitude A_n to the parameters of the system. Here, we obtain

$$A_n^2 = \frac{4\Gamma^{3/2}(\phi - \phi_n)(K^2 + 3\Gamma n^2)(K^2 - \Gamma n^2)^{1/2}}{(12 - 7\Gamma)K^4 + 2n^2\Gamma^2(1 - 2\Gamma)K^2 - 3n^4\Gamma^3}.$$

So far, we have discussed the bifurcation of a straight filament at the onset of instability. In order to complete the description of the problem, it is of interest to describe other possible solutions of the system and their elastic energy, namely, the helicoidal solutions that are found asymptotically in the perverted tendril. There is, in fact, a family of such solutions for every given value of the tension, parametrized by the Frenet curvature:

$$\kappa = (0, \kappa_F, \tau_F) \qquad f = \left(0, f_0, \frac{\tau_F}{\kappa_F}f_0\right), \tag{11}$$

where $f_0 = -\tau_F(\kappa_F - K) + \Gamma\kappa_F\tau_F$. The tension $\phi^2 = f_3$ sets the torsion: $\tau_F^2 = \phi^2\kappa_F/[K + \kappa_F(\Gamma - 1)]$. The lowest energy states correspond to the helices with (κ_F, τ_F) such that $2(\Gamma - 1)\kappa_F^3 - 2K(\Gamma - 2)\kappa_F^2 - 2\kappa_F K^2 + \Gamma\tau_F^2 K = 0$. In the (κ_F, τ_F) plane, this family of *optimal solutions* forms a closed curve passing through the points $(0,0)$ (straight line) and $(K,0)$ (rings). Each point on the curve represents an optimal helix for given ϕ, K, Γ. The perverted filament connects asymptotically two optimal helices [a right-handed one ($\tau_F > 0$) to a left-handed one ($\tau_F < 0$)].

The twist contained in a half filament for given intrinsic curvature and tension can be obtained by assuming that this half filament is well represented by an optimal helix; then the total twist Tw is given by the number of helical repeats (holding the ends, the total twist is the twist obtained by pulling the helix to a straight filament, converting helical torsion to twist density):

$$Tw^2 = \frac{L^2}{4}\left(\kappa_F^2 + \frac{\phi^2\kappa_F}{K + \kappa_F(\Gamma - 1)}\right), \tag{12}$$

where κ_F is the curvature of the optimal solution with given tension ϕ^2.

The energetic and stability analysis can now be used together to give a complete picture of the mechanics and dynamics of tendril perversion. For a given intrinsic curvature as the tension decreases (or equivalently for given tension and increasing intrinsic curvature), the straight tendril reaches a critical state where it loses stability. Right at the onset of instability, the filament is well described by the solutions given by the stability analysis. As the tension is further decreased, the central piece is still best described by the same nonlinear solutions whereas the long range solutions (the asymptotic states) are described by the helical solutions obtained by energetic consideration. In Fig. 2, we show the closed curve of optimal solutions in the (κ_F, τ_F) plane. A perverted tendril will connect two asymptotic states with opposite hands (represented by two circles for a specific value of the tension) joined by the central piece given by the stability analysis. The perverted filament is a heteroclinic orbit in the curvature-torsion plane joining two asymptotic fixed points (the helices).

The perversion of tendrils in climbing plants provides a remarkable answer to an elementary mechanical question, namely: How does one build a twistless spring? As

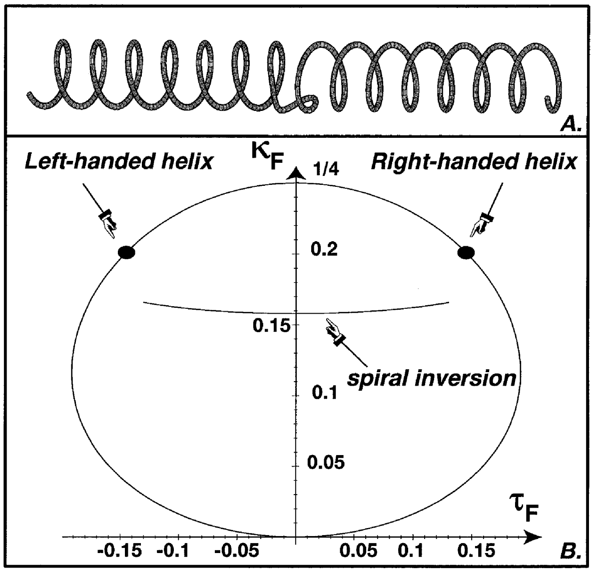

FIG. 2. (*A*) Sketch of a helix hand reversal. (*B*) The optimal solution curves in the $\tau_F - \kappa_F$ plane together with the two optimal helices (circles) obtained for $K = 1/4$, $\Gamma = 3/4$, $n = 1/8$, and $\phi = \phi_2 \approx 0.286$. The inside curve is the one obtained by the nonlinear analysis for the central piece.

shown here, the twistless spring can be simply created by a change in intrinsic curvature. The structure that results is a coupling of two (or more) helical springs with opposite handedness. The modeling of this phenomenon through Kirchhoff's theory of thin rods provides quantitative results on the critical parameters involved in the process, as well as a complete qualitative picture of the mechanism involved. It also highlights an intriguing scenario for morphogenesis where local curvature, rather than twist, determines the final structure. The remarkable feature of this mechanism is the existence of a global invariant (the total twist) which is conserved in the symmetry breaking bifurcation.

This work is supported by the Flinn Foundation, NSF Grant No. DMS-9704421, and the NATO-CRG program.

*Electronic address: agoriel@ulb.ac.be

[1] N. H. Mendelson, Proc. Natl. Acad. Sci. U.S.A. **75**, 2472–2482 (1978).

[2] R. L. Ricca, J. Phys. A **28**, 2335–2352 (1995); J. M. T. Thompson and A. R. Champneys, Proc. R. Soc. London A **452**, 117–138 (1996).

[3] Ch. Darwin, *The Movements and Habits of Climbing Plants* (D. Appleton, New York, 1888).

[4] *Mechanics of Flexible Fibre Assemblies,* edited by J. W. S. Hearle, J. J. Thwaites, and J. Amirbayat (Sijthoff & Noordhoff, Alphen aan den Rijn, The Netherlands, Germantown, MD, 1980).

[5] L. Waterkeyn, in *Cotton Fibres: Their Development and Properties* (International Institute for Cotton, Manchester, UK, 1985), pp. 17–22.

[6] M. J. Tilby, Nature (London) **266**, 450–552 (1977).

[7] J. W. Galloway, in *Biological Asymmetry and Handedness* (Wiley-Interscience, New York, 1991).

[8] E. H. Dill, Arch. Hist. Exact. Sci. **44**, 2 (1992); B. D. Coleman *et al.,* Arch. Ration. Mech. Anal. **121**, 339 (1993).

[9] A. Goriely and M. Tabor, Phys. Rev. Lett. **77**, 3537–3540 (1996); Physica (Amsterdam) **105D**, 20–44 (1997); Physica (Amsterdam) **105D**, 45–61 (1997); "Nonlinear Dynamics of Filaments III: Instabilities of Helical Rods," Proc. R. Soc. London A (to be published).

[10] A. Goriely and M. Tabor, "Nonlinear Dynamics of Filaments IV: Spontaneous Looping," Proc. R. Soc. London A (to be published).

[11] J. Sachs, *Text-book of Botany, Morphological and Physiological* (Clarendon Press, Oxford, 1875).